Research Repository

A network anatomy of cross-currency basis swap spreads: evidence from 25 currencies

Accepted for publication in the European Journal of Finance

https://doi.org/10.1080/1351847x.2026.2723814

A Network Anatomy of Cross-Currency Basis Swap Spreads: Evidence from 25 Currencies

Daniel Felix Ahelegbey[a], Oyakhilome Wallace Ibhagui[b,*], Florian Gerth[c]

[a] *University of Essex, School of Mathematics, Statistics, and Actuarial Science, UK*
[b] *BAUM TenPers Research Institute, Virginia, USA*
[c] *ISM University of Management and Economics, Lithuania*

Abstract

We develop a novel network-based framework that treats cross-currency basis swap spreads as reflecting currency- and tenor-specific inventory frictions, cross-linkages of currencies on shared balance sheets, and global funding tightness that spikes during crises. The framework delivers several theoretical predictions that anchor our empirical analysis: (i) basis spreads for USD-pegged currencies exhibit muted volatility and rarely transmit shocks; (ii) longer-tenor bases display lower volatility and weaker spillovers than their short-tenor counterparts; (iii) crisis episodes amplify comovement across currencies; and (iv) spillover transmission is governed by structural centrality within the dealer-linkage network. We test these predictions using cross-currency basis swap spreads across 25 currencies (the largest empirical study of its kind), estimated via a Bayesian graphical SVAR that uncovers a sparse, directed spillover network. The evidence supports all four theoretical predictions: pegged currencies remain insulated and transmit minimal shocks; volatility and contagion diminish with maturity; interconnectedness surges during crises; and the transmission of shocks is Euro-centred, with the Swiss franc and Danish krone closely following the Euro in systemic importance.

Keywords: Covered Interest Parity, Cross-currency Basis Swap Spreads, Currency Swaps, Dollar Funding, Financial Crisis, Interconnectedness, VAR Model.

JEL: C11, C32, F31, G01, G15

1. Introduction

A cross-currency basis measures the cost difference between borrowing a currency directly and obtaining it synthetically through the swap market. Under Covered Interest Parity (CIP), these costs should be equal, yet the basis often deviates from zero, signalling funding imbalances. Such deviations were negligible before 2007 for most currencies, but surged during the 2007–2009 global financial crisis, re-emerged during the 2010–2013 Eurozone crisis, widened again amid the 2015–2018 geopolitical tensions, and resurfaced during the COVID-19 pandemic. Figure 1 illustrates this evolution of the average U.S. dollar (USD) cross-currency basis for the G-10 currencies.

*Corresponding author

Email addresses: d.f.ahelegbey@essex.ac.uk (Daniel Felix Ahelegbey), wallace@aims.ac.za (Oyakhilome Wallace Ibhagui), flo.gerth@web.de (Florian Gerth)

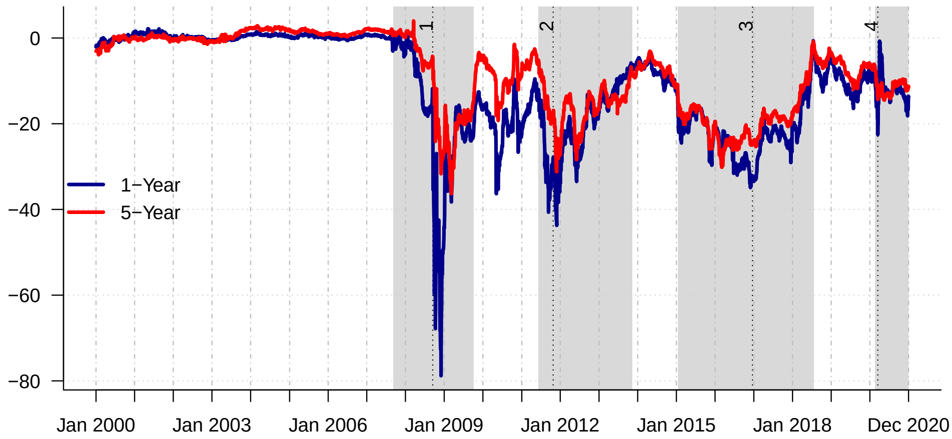

Figure 1: Averaged G-10 cross-currency basis swap spreads with 1-& 5-year maturities (Jan 2000 – December 2020). Grey-shaded regions correspond to 1) 2007–2009, 2) 2010–2013, 3) 2015–2018, and 4) 2020.

Persistent CIP deviations have therefore made the basis a state-dependent indicator of global USD funding stress. The major disruptions over the past two decades have altered long-standing financial relationships and increased market segmentation, amplifying the transmission of shocks across currencies (Abakah et al., 2024; Cerutti and Zhou, 2024; Eguren-Martin et al., 2024). These developments highlight the importance of understanding how funding pressures and cross-currency interdependence jointly shape deviations from CIP.

Studies on deviations from CIP span several decades. Early work by Callier (1981) showed that transaction costs and market frictions could generate small, temporary violations of CIP, laying the groundwork for understanding conditions under which parity might fail to hold exactly. The global financial crisis of 2007–2009 marked a turning point. Seminal studies by Baba et al. (2008), Baba and Packer (2009a), and Baba and Packer (2009b) documented large and persistent CIP deviations during this period, attributing them to heightened counterparty risk and acute shortages of USD liquidity that impaired the functioning of the cross-currency swap market.

Following the financial crisis, research expanded substantially to explain the underlying drivers and persistence of CIP deviations. Studies by Coffey et al. (2009), Fong et al. (2010), and Hui et al. (2011) emphasised the role of regulatory changes and balance-sheet constraints in sustaining these deviations. Du and Schreger (2016) showed that even at very short maturities, CIP violations created economically meaningful arbitrage opportunities, challenging classical limits-of-arbitrage theories such as Shleifer and Vishny (1997). Extending this analysis, Du et al. (2018) documented strong relationships between CIP deviations, fixed-income spreads, and nominal interest rates, highlighting the importance of intermediary balance-sheet frictions in shaping cross-currency funding conditions. More recently, Ben Zeev and Nathan (2024) emphasised that demand-side factors, particularly the effects of Basel III and related macroprudential regulations, created frictions in financial intermediation efficiency that contributed to persistent CIP deviations. Finally, Cunado et al. (2024), in a study spanning more than two centuries, argued that the breakdown of no-arbitrage conditions exhibits important historical regularities linked to periods of financial stress and market fragmentation.

A related strand of the literature highlights the role of Federal Reserve interventions, especially swap-line extensions to foreign central banks, in mitigating stresses in global USD funding markets. Notable contributions include Baba and Packer (2009a), Aizenman and

Pasricha (2010), Avdjiev et al. (2020), Stenfors et al. (2022), and Geyikci and Özyildirim (2023). Avdjiev et al. (2019a) and Cerutti et al. (2021) examined macro-financial factors influencing CIP deviations, demonstrating how broader economic and financial conditions affect cross-currency basis swap spreads. Additionally, Ibhagui (2019) provided evidence that inflation differentials contribute to cross-currency basis swap spreads. Finally, Aizenman et al. (2022) argued that major central banks can alleviate acute strains in offshore USD funding markets through coordinated liquidity provision.

Despite these important advances, several key issues remain insufficiently understood. First, much of the existing literature focuses primarily on the determinants and persistence of bilateral CIP deviations, while paying comparatively limited attention to the network structure through which funding shocks propagate across currencies. Although prior studies establish the importance of dealer balance-sheet constraints, regulatory frictions, and global USD shortages, less is known about how these forces jointly generate systemic spillovers and contagion within the broader cross-currency basis market.

Consistent with Avdjiev et al. (2019b), financial interconnectedness implies that stress originating in one segment of the global financial system may propagate through direct and higher-order financial linkages. Importantly, they distinguish contagion from simple interdependence, highlighting that common co-movement need not itself constitute contagion. This distinction is particularly relevant for cross-currency basis markets, where correlated movements may reflect either common exposure to global USD funding conditions or genuine propagation through interconnected funding channels.

Second, existing empirical evidence focuses heavily on a relatively narrow set of developed-market currencies, particularly the G-10, while the interconnected dynamics between developed and emerging-market currencies remain underexplored. This limitation has become increasingly important because recent episodes of financial stress have shown that offshore USD funding pressures now propagate rapidly across both advanced and emerging economies through globally interconnected dealer balance sheets.

Third, although prior studies document that CIP deviations intensify during crisis episodes, there remains limited evidence on how contagion dynamics vary across maturities, how network centrality shapes the transmission of funding shocks, and why some currencies—particularly currencies with exchange-rate pegs to the USD—appear relatively insulated from global funding disruptions. Understanding these mechanisms is important because modern offshore USD funding markets increasingly operate as tightly interconnected systems in which stress originating in one segment can rapidly spill over into others.

While stronger co-movement during crises, the prominence of major funding currencies, and the relative insulation of pegged currencies are broadly consistent with established findings in the CIP literature, the network perspective provides information that cannot be obtained from standard correlation analysis or factor models. Unlike these approaches, the network framework identifies directional propagation and heterogeneous transmission channels across currencies, allowing us to distinguish between net transmitters and receivers of funding stress and to characterize how the topology of the system evolves across maturities and crisis episodes. Consequently, the network approach provides a richer characterization of systemic funding risk than can be inferred from average co-movement alone.

The theoretical framework therefore implies that network centrality and directional spillovers contain information beyond average co-movement and provide a testable distinction between systemic propagation and common-factor exposure.

Taken together, the existing studies have substantially improved our understanding of why

CIP deviations arise and persist. However, it provides less evidence on how funding shocks propagate across currencies as an interconnected network. Understanding these spillover dynamics is increasingly important because modern offshore USD funding markets are characterised by globally integrated dealer balance sheets, rapid cross-market transmission of stress, and recurrent episodes of synchronised funding dislocations. These considerations motivate the need for a framework capable of jointly analysing contagion, currency centrality, maturity heterogeneity, and crisis amplification in cross-currency basis swap markets.

To study these interconnected spillover dynamics, we employ the Bayesian graphical structural vector autoregressive (BGSVAR) model (Ahelegbey et al., 2016), a network-based framework that captures both contemporaneous and lagged spillovers across currencies while effectively addressing the high dimensionality inherent in global funding markets.

Against this backdrop, our study focuses on three main questions: (1) Do movements in cross-currency basis swap spreads reflect systemic contagion across currencies? (2) Which currencies occupy central positions in transmitting funding shocks through the foreign exchange derivatives market? and (3) How do cross-currency spillover dynamics vary across maturities and exchange-rate regimes?

Our study makes three contributions. First, we present a dealer-intermediary framework that microfounds the interconnected behaviour of cross-currency basis swap spreads. The model shows how dealer balance-sheet constraints, cross-currency funding linkages, and global USD funding tightness jointly generate contagion, crisis amplification, maturity heterogeneity, and differences in spillover transmission across currencies. The framework additionally generates empirically testable predictions regarding the role of network centrality and the relative insulation of currencies with tighter exchange-rate pegs to the USD.

Second, using data for 25 major currencies against the USD, we provide new evidence that cross-currency basis markets behave as highly interconnected funding networks during periods of stress. Our results show that contagion intensifies sharply during crisis episodes and that spillover transmission is concentrated around a small set of structurally central currencies, particularly the Euro, Swiss franc, and Danish krone. These findings directly address whether CIP deviations reflect systemic contagion rather than isolated currency-specific dislocations.

Third, we document substantial heterogeneity in the transmission of funding shocks across maturities and exchange-rate regimes. Short-tenor basis spreads exhibit stronger contagion and higher volatility, whereas longer-tenor spreads are more stable and less interconnected. In addition, currencies with tighter exchange-rate pegs to the USD display comparatively muted spillover dynamics during crisis periods. Together, these findings provide new evidence on how market structure and dealer balance-sheet frictions shape the propagation of global USD funding stress.

The remainder of the paper is organised as follows. Section 2 presents the theoretical framework. Section 3 introduces the Bayesian network-VAR methodology. Section 4 describes the data. Section 5 reports the empirical findings, and Section 6 concludes.

2. Theoretical Foundations

We develop a tractable theoretical framework that rationalises the interconnected behaviour of cross-currency basis swap spreads (CCBS). The model microfounds how contagion, currency centrality, and heterogeneity across pegged and long-tenor currencies emerge from intermediary frictions and heterogeneous client demand. In doing so, it provides the structural underpinnings for the empirical propositions tested in Section 5.

2.1. Model Setup

Consider n currencies indexed by $k \in \{1, \dots, n\}$ over periods $t = 0, 1, 2, \dots$. For each currency k, let $b_{k,t}$ denote its deviation from covered interest parity (CIP), and collect all basis spreads in the vector $b_t = (b_{1,t}, \dots, b_{n,t})'$.

Global clients demand USD funding against foreign currency k. Let $d_{k,t} > 0$ denote net USD demand (and $d_{k,t} < 0$ net USD supply), and define $d_t = (d_{1,t}, \dots, d_{n,t})'$., the total client USD demand across currencies.

Dealers stand on the opposite side of these flows and must absorb the net USD imbalances. Let $q_t = (q_{1,t}, \dots, q_{n,t})'$ denote dealer USD supply across currencies. Dealers are therefore the intermediaries that clear imbalances in USD demand across currencies, and the cost of intermediation gives rise to the observed structure of cross-currency basis spreads.

Following the dealer-intermediation literature e.g., Garleanu and Pedersen (2011), He and Krishnamurthy (2013), and Duffie (2010), absorbing client order flow entails convex balance-sheet costs. The total cost of warehousing positions is

$$C_t(q_t) = \tfrac{1}{2}\, q_t' \Big(T + \Phi + \Lambda_t \mathbf{1}\mathbf{1}'\Big) q_t,$$

where the matrix $T = \mathrm{diag}(\tau_1, \dots, \tau_n)$ captures currency- and maturity-specific inventory costs. A higher τ_k indicates that taking on an additional unit of exposure in currency k puts more pressure on dealer balance sheets. The matrix $\Phi = (\phi_{ij})$ is symmetric with $\phi_{ij} \geq 0$ and reflects cross-currency balance-sheet linkages, meaning warehousing currency i uses similar funding channels as currency j, making their marginal costs interdependent. Finally, the parameter $\Lambda_t \geq 0$ represents global funding tightness. The rank-one component $\Lambda_t \mathbf{1}\mathbf{1}'$ imposes a common surcharge across all positions and rises sharply during episodes of systemic stress, consistent with evidence in Borio et al. (2016) and Du et al. (2018).

Dealers are risk-neutral and competitive, so zero-profit pricing implies that basis spreads equal marginal costs. Differentiating the cost function yields:

$$b_t = \nabla_{q_t} C_t(q_t) = (T + \Phi + \Lambda_t \mathbf{1}\mathbf{1}') q_t.$$

For convenience, define the composite cost kernel

$$K_t \equiv T + \Phi + \Lambda_t \mathbf{1}\mathbf{1}',$$

which summarises the balance-sheet frictions relevant for equilibrium basis formation. The diagonal elements of K_t combine currency- and maturity-specific inventory costs (τ_k) with the systemic surcharge Λ_t, determining the marginal cost of absorbing additional exposure in each currency. The off-diagonal elements capture: (i) bilateral balance-sheet linkages ϕ_{ij}, which transmit costs across currency pairs, and (ii) the global stress component Λ_t, which raises comovement during crises. Thus, K_t acts as the "pricing kernel" of the dealer sector.

Using the market-clearing condition $q_t = d_t$, we obtain the equilibrium pricing relation

$$b_t = \nabla_{q_t} C_t(q_t)\big|_{q_t = d_t} = (T + \Phi + \Lambda_t \mathbf{1}\mathbf{1}') d_t \equiv K_t d_t, \tag{1}$$

In tranquil periods, K_t is dominated by T and Φ, so basis spreads primarily reflect idiosyncratic inventory costs and bilateral linkages. In periods of systemic stress, Λ_t increases sharply, tilting K_t toward a near-rank-one structure and enforcing strong co-movement across all basis spreads. This mechanism explains why CIP deviations, which appear heterogeneous in normal times, suddenly synchronise during global funding disruptions.

Although our framework emphasises dealer balance-sheet constraints as a source of synchronisation, periods of global stress are also characterised by simultaneous increases in demand for USD funding and hedging across currencies. Consequently, heightened interconnectedness may reflect the joint interaction of intermediary constraints and synchronised demand pressures rather than supply-side forces alone.

The quadratic cost specification ensures convexity, meaning marginal costs rise with position size. This captures risk-management constraints and regulatory capital charges common in the intermediated funding environment.

Three economic mechanisms follow from this equilibrium structure. First, inventory frictions[1], represented by T, ensure that basis spreads rise with the intensity of demand, with larger effects in currencies or maturities with higher inventory costs. Second, cross-currency linkages captured by Φ transmit shocks across currencies: a large ϕ_{ij} indicates that demand pressure in currency i generates spillovers into currency j through shared balance-sheet constraints. Third, systemic stress captured by Λ_t produces global co-movement during crises; even idiosyncratic demand shocks can generate widespread widening of basis spreads when Λ_t rises, explaining the surge in cross-currency correlations observed empirically.

In short, (1) shows that CIP deviations represent the shadow prices of dealer balance-sheet usage. The matrix K_t fully characterises how client USD demand propagates through the intermediation sector to generate the observed network of basis spreads.

2.2. Testable Propositions

The theoretical framework provides a set of predictions that guide the empirical analysis. These propositions characterise how systemic stress, balance-sheet linkages, and inventory frictions shape the behaviour of cross-currency basis swap spreads.

Proposition 1 (Contagion Amplification)**.** *As Λ_t rises during crises, cross-currency basis swap spreads become increasingly interconnected. In the limit as $\Lambda_t \to \infty$, their pairwise correlations converge to unity. See Appendix A.1 for formal derivation.*

This reflects the role of Λ_t as a global funding stress parameter. When USD scarcity rises, the marginal cost of supplying USD increases uniformly across markets, effectively binding currencies through a common factor. As a result, basis spreads co-move strongly in crises, and idiosyncratic currency differences are dominated by global scarcity of USD liquidity.

Proposition 2 (Currency Centrality)**.** *Define the centrality of currency k in the network as*

$$C_k = \sum_{j \neq k} \phi_{kj} \tag{2}$$

[1]Inventory friction refers to the balance-sheet resistance to the provision of synthetic dollars that arises when dealers are forced to warehouse rather than immediately offset FX swap positions. In such situations, intermediaries must commit scarce capital and absorb the associated risks, which becomes increasingly costly when regulatory constraints are binding. The resulting expansion of balance-sheet usage reduces the capacity available for further intermediation and limits dealers' ability to provide additional synthetic dollars. Consequently, synthetic dollar funding becomes more expensive, contributing to dollar scarcity and wider cross-currency basis spreads.

A currency k is a central transmitter of shocks if

$$C_k > C_i \qquad \forall i \neq k \tag{3}$$

See Appendix A.2.

The matrix Φ encodes the network of cross-currency spillovers. A shock to currency k propagates to all others with weights ϕ_{kj}. Currencies with large C_k occupy structurally important positions in the dealer balance-sheet network. They function as "super-spreaders" of shocks, transmitting liquidity disturbances widely through the system.

Proposition 3 (Pegged Currency Immunity)**.** *If currency k is tightly pegged to USD, so that its idiosyncratic net USD demand and bilateral balance-sheet linkages are negligible, then its basis is driven primarily by the common stress component and therefore remains comparatively muted even during crises.*

Pegged currencies exhibit little independent hedging or speculative demand, since their exchange rate risk relative to USD is contractually or institutionally suppressed. As a result, their basis spreads remain stable even when systemic shocks propagate elsewhere. This is consistent with their weak participation in contagion dynamics.

Proposition 4 (Maturity Heterogeneity)**.** *If inventory costs increase with maturity and long-tenor demand and cross-currency propagation are sufficiently damped relative to short-tenor demand and propagation, then longer-tenor basis spreads are less volatile and exhibit weaker spillover dynamics than short-tenor spreads.*

Inventory costs τ_k rise with tenor because long-maturity positions tie up dealer balance sheets for extended periods. In equilibrium,

$$b_t = (T + \Phi + \Lambda_t \mathbf{1}\mathbf{1}')d_t$$

At short maturities, τ_k is small, so spreads are dominated by cross-currency linkages (Φ) and systemic stress (Λ_t), generating strong comovement and high volatility. At longer maturities, larger τ_k values cause local absorption costs to dominate, muting spillovers and smoothing volatility. Thus, long-tenor basis spreads appear more stable and idiosyncratic, while short-tenor spreads display stronger contagion.

3. Bayesian Graphical SVAR Methodology

This section outlines the Bayesian Graphical SVAR framework used to analyse the contagion dynamics of the basis. The methodology integrates a structural VAR representation with a graphical model that induces sparsity and uncovers the underlying network structure.

3.1. Structural Vector Autoregressive Model

Let $Y_t = (Y_{1,t}, \dots, Y_{n,t})'$ denote an n-dimensional vector of variables. The structural VAR(p) model is written as

$$Y_t = B_0 Y_t + B_1 Y_{t-1} + \cdots + B_p Y_{t-p} + \varepsilon_t, \qquad \varepsilon_t \sim \mathcal{N}(0, \Sigma), \tag{4}$$

where p is the lag order, B_0 captures contemporaneous relationships, $B_1, \dots, B_p$ describe dynamic interactions, and the structural shocks ε_t are mutually uncorrelated.

Direct estimation of (4) is hindered by simultaneity in $B_0 Y_t$, high dimensionality, and the non-identifiability of structural shocks from the reduced-form representation alone. These challenges motivate the use of a sparse representation that recovers the structural parameters.

3.2. Bayesian Graphical SVAR Model

The BGSVAR (Ahelegbey et al., 2016) addresses SVAR identification and overparameterisation by assigning to each coefficient $B_{ij,s}$, a binary indicator $G_{ij,s} \in \{0, 1\}$ such that

$$B_{ij,s} = \begin{cases} \beta_{ij,s}, & \text{if } G_{ij,s} = 1, \\ 0, & \text{if } G_{ij,s} = 0, \end{cases} \qquad G_{ij,s} = \begin{cases} 1, & \text{if } Y_{j,t-s} \to Y_{i,t} \\ 0, & \text{otherwise} \end{cases} \tag{5}$$

where $Y_{j,t-s} \to Y_{i,t}$ indicates a directed contemporaneous ($s = 0$) or dynamic ($s \geq 1$) effect.

This formulation induces sparsity and yields a parsimonious representation of the underlying network structure. In this framework, contemporaneous edges arise from non-zero coefficients in B_0; dynamic edges arise from non-zero coefficients in $B_1, \dots, B_p$. This imposes structural zeros, reduces overfitting, and stabilises inference in high-dimensional settings.

3.3. Prior Specification

To induce sparsity, we assign priors jointly on coefficients and selection indicators:

$$[B_{ij,s} \mid G_{ij,s} = 1] \sim \mathcal{N}(0, \eta), \qquad G_{ij,s} \sim \text{Ber}(\pi_{ij}), \qquad \sigma_i^2 \sim \text{InvGamma}(\nu, \delta)$$

where η controls the shrinkage of coefficients. When $G_{ij,s} = 1$, the coefficient $B_{ij,s}$ follows a Gaussian prior. Edges in $G_{ij,s}$ are Bernoulli distributed with π_{ij} as the prior probability of a link. Structural shocks are assumed to be mutually independent, with independent inverse-Gamma priors to the variances, where ν and δ are shape and scale parameters, respectively.

3.4. Posterior Approximation

Posterior inference is based on the joint distribution of $(B_0, B_{1:p}, G_{0:p}, \Sigma)$. The posterior inclusion probability $P(G_{ij,s} = 1 \mid \text{Data})$ quantifies the likelihood for each directed link. We employ a collapsed Gibbs sampler that cycles through the conditionals:

$$P(G_{1:p} \mid Y, p), \quad P(G_0 \mid Y, p, \hat{G}_{1:p}), \quad P(B_0, B_{1:p} \mid Y, p, \hat{G}_{1:p}, \Sigma), \quad P(\Sigma \mid Y, p, \hat{G}, \hat{B})$$

This sampler exploits conditional conjugacy, improving mixing and computational efficiency. In our implementation, we set $\pi_{ij} = 0.5$, $\eta = 100$, and $\nu = \delta = n + 2$.

3.5. Network Construction

Posterior estimates of the network produce posterior inclusion probabilities (PIPs). Statistically significant links can then be identified by thresholding the PIP at level $\alpha = 0.5$:

$$\widehat{B}_{ij,s} = \begin{cases} \hat{\beta}_{ij,s}, & P(G_{ij,s} = 1) \geq \alpha, \\ 0, & \text{otherwise.} \end{cases}$$

From these coefficients, we construct a binary, A, and a weighted adjacency matrix, W:

$$A_{ij} = \mathbf{1}\left(\sum_{s=0}^{p} \widehat{B}_{ij,s} \neq 0\right), \qquad W_{ij} = \sum_{s=0}^{p} \widehat{B}_{ij,s}$$

where A_{ij} captures the presence of any contemporaneous or lagged connection from $j \to i$, and W_{ij} measures aggregate directional influence.

3.6. Network Metrics

To summarise interconnectedness, we compute standard systemic-risk network indicators using the adjacency matrix A. We focus on network density and hub/authority centrality.

Network Density: the proportion of active connections:

$$\text{Density}(A) = \frac{1}{n(n-1)} \sum_{i \neq j} A_{ij}.$$

Hub and Authority Centrality: hubs point to important nodes, and authorities are nodes pointed to by strong hubs:

$$(A'A)h_u = \lambda_h^u h_u, \qquad (AA')a_u = \lambda_a^u a_u.$$

Network-Based Turbulence Index: To measure systemwide market stress, we compute a turbulence index that combines individual asset volatilities with network amplification effects. Let $Y = (Y_1, \dots, Y_n)'$ be daily returns and let $\sigma(Y)$ denote their standard deviations. Define

$$\Omega = (I + W)'(I + W),$$

which captures how volatilities are propagated through network linkages. The network-based turbulence index is then given by (Ahelegbey and Giudici, 2022):

$$T^{sys} = \sqrt{\frac{1}{n} \sigma(Y)' \, \Omega \, \sigma(Y)}$$

Higher values of T^{sys} indicate periods with elevated price fluctuations and strong transmission across the network, signalling systemic turbulence.

4. Data Description

Existing studies on cross-currency basis swaps (CCBS) have mostly focused on the G-10 currencies. However, recent events have shown a shift in the ranking of currencies, with some G-10 members gradually losing their status as developed market currencies. Prominent among such currencies is the British pound (GBP), traditionally part of the G-5 currency group, which has seen its status affected by events like Brexit, making it more akin to an emerging market currency. Conversely, some emerging market currencies[2] are gradually gaining quasi-developed market status due to their resilience during events such as the COVID-19 pandemic.

[2] See https://www.refinitiv.com/perspectives/market-insights/how-hard-has-covid-19-hit-em-currencies/

We utilise daily data from Bloomberg from January 2000 to December 2020 and compare 25 major funding currencies (G-25) to the U.S dollar (USD). Our G-25 consists of 13 developed and 12 emerging economies, following the Morgan Stanley Capital International Market Classification. See Table 1 for a description of the currencies.

Market	No.	Country/Region	Currency	CCB	Start Date	End Date
Developed	1	Euro Area	Euro	EUR	3/1/2000	31/12/2020
	2	Japan	Japanese yen	JPY	3/1/2000	31/12/2020
	3	United Kingdom	British pound	GBP	3/1/2000	31/12/2020
	4	Australia	Australian dollar	AUD	3/1/2000	31/12/2020
	5	New Zealand	New Zealand dollar	NZD	3/1/2000	31/12/2020
	6	Canada	Canadian dollar	CAD	3/1/2000	31/12/2020
	7	Denmark	Danish krone	DKK	3/1/2000	31/12/2020
	8	Switzerland	Swiss franc	CHF	3/1/2000	31/12/2020
	9	Sweden	Swedish krona	SEK	3/1/2000	31/12/2020
	10	Norway	Norwegian krone	NOK	3/1/2000	31/12/2020
	11	Israel	Israeli shekel	ILS	3/7/2011	31/12/2020
	12	Hong Kong	Hong Kong dollar	HKD	3/1/2000	31/12/2020
	13	Singapore	Singapore dollar	SGD	3/1/2000	31/12/2020
Emerging	14	Thailand	Thai baht	THB	26/6/2006	31/12/2020
	15	Malaysia	Malaysian ringgit	MYR	9/5/2005	31/12/2020
	16	Korea	Korean won	KRW	26/2/2003	31/12/2020
	17	Russia	Russian ruble	RUB	2/11/2006	31/12/2020
	18	South Africa	South African rand	ZAR	3/1/2000	31/12/2020
	19	Turkey	Turkish lira	TRY	19/9/2006	31/12/2020
	20	UAE	UAE dirham	AED	14/8/2009	31/12/2020
	21	Saudi Arabia	Saudi riyal	SAR	27/11/2009	31/12/2020
	22	Chile	Chilean peso	CLP	24/4/2009	31/12/2020
	23	Mexico	Mexican peso	MXN	24/2/2000	31/12/2020
	24	China	Chinese yuan	CNY	21/7/2009	31/12/2020
	25	Qatar	Qatari riyal	QAR	27/8/2012	31/12/2020

Table 1: The major 25 world cross-currencies grouped according to the MSCI Market Classification.

A small number of currencies require special treatment because market conventions differ across jurisdictions. In particular, CLP and MXN basis quotes are conventionally expressed on the USD leg, whereas the remaining currencies in the sample are quoted on the non-USD leg. To ensure comparability and maintain a consistent interpretation across the panel, we multiply the CLP and MXN basis series by -1, thereby aligning their sign convention with that used for the other currencies. This transformation preserves the underlying information contained in the basis spreads and facilitates the interpretation of network centrality measures and spillover dynamics across currencies.

In Figure 2, we report the time series of the CCBS for the G-25 currencies grouped according to developed and emerging markets with 1- and 5-year maturities. We notice that between 2000 and 2006, most of the basis spreads were generally within the neighbourhood of zero. This suggests that in the years preceding the global financial crisis (GFC), any CIP rule held approximately, and any deviation was quickly arbitraged away because USD was more readily available to market participants. The supply of USD funding was hardly ever constrained, as there was the absence or diminished presence of any financial intermediation channel, and neither USD funding specialness nor foreign currency specialness existed.

During the crisis of 2007–2009, the CCBS showed significant pickups in the CIP deviations,

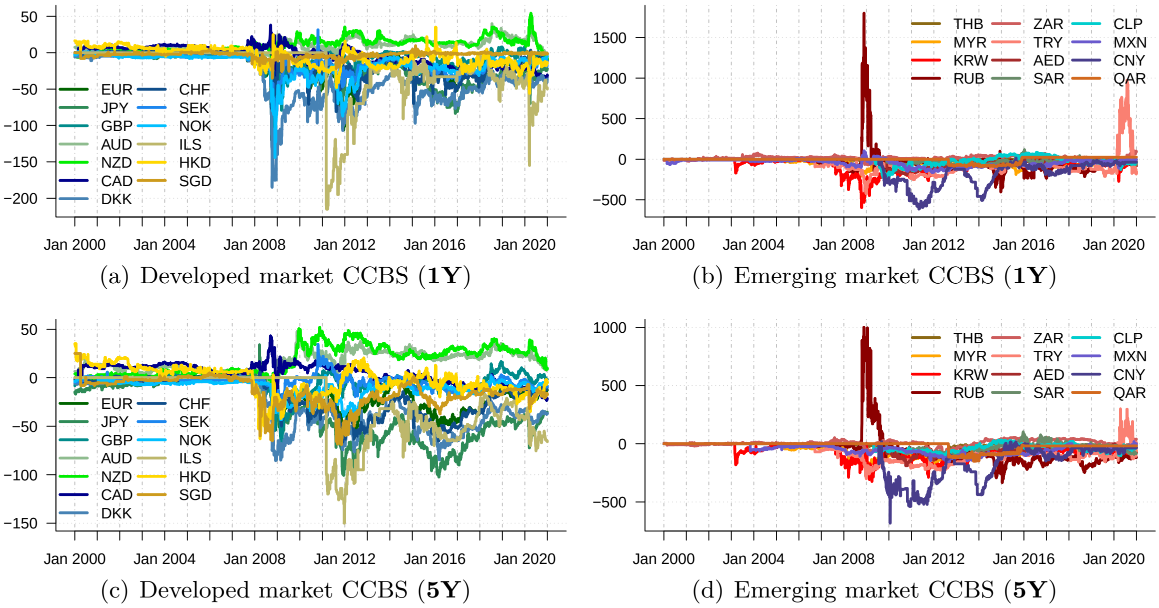

(a) Developed market CCBS (**1Y**)

(b) Emerging market CCBS (**1Y**)

(c) Developed market CCBS (**5Y**)

(d) Emerging market CCBS (**5Y**)

Figure 2: Time series of Cross-currency basis swaps (Jan 2000–December 2020).

most of which were negative. During this period, the supply of USD funding was highly constrained, an intense USD funding specialness emerged, financial intermediaries became more constrained, and a strong presence of a financial intermediation channel arose.

The timeline of events shows that during the GFC, non-US entities (foreign financial institutions with interests in the US) needed USD to fund their US operations. However, these institutions were unable to access the USD cash market directly because US financial institutions were concerned about counterparty risk. As a result, these non-US entities turned to the cross-currency swap market, where they swapped non-USD currency for USD. This raised the cost of synthetic USD in the swap market due to the high demand for USD hedges relative to the supply of USD hedges. The higher cost of synthetic USD in cross-currency swap markets forced foreign entities to pay a premium (compared to the cost of raising direct USD in the cash market), which led to what we know today as cross-currency basis swap spreads. In 2010–2013, during the Eurozone crisis, the basis spreads widened again, albeit to a lesser extent compared to the GFC.

Table 2 presents the statistics of the basis spreads over three crisis periods: 2007–2009, 2010–2013, and 2020. According to the table, the most volatile basis during the three crisis periods is usually from emerging market currencies. For both 1- and 5-year maturity basis, the Russian ruble (RUB) recorded the highest standard deviation of 321.6 between 2007–2009, the Chinese yuan (CNY) recorded the highest volatility between 2010–2013, and the Turkish lira (TRY) topped the list of the most volatile in 2020. Among the developed market currencies, the Danish krone (DKK) was the most volatile in 2007–2009, while the Israeli shekel (ILS) topped the list between 2010–2013 and 2020.

During the crisis periods shown in Table 2, as well as in the pre-and post-crisis periods illustrated in Figure 2, the basis for the AUD and NZD remained positive even when others became strongly negative. This implies that while other non-US entities were paying a premium to obtain (synthetic) USD in the swap market, the AUD and NZD entities could

	1-Year Maturity CCBS			5-Year Maturity CCBS		
	2007–2009	2010–2013	2020	2007–2009	2010–2013	2020
EUR	-21.4 (23.0)	-35.7 (19.9)	-11.1 (4.2)	-14.8 (16.2)	-29.6 (11.9)	-16.6 (4.0)
JPY	-14.2 (15.1)	-28.0 (9.4)	-29.9 (9.6)	-13.5 (20.1)	-58.5 (15.4)	-46.1 (8.4)
GBP	-20.8 (22.4)	-8.5 (7.1)	-2.3 (3.4)	-17.1 (18.1)	-7.1 (7.6)	-0.4 (3.3)
AUD	6.2 (9.1)	10.8 (6.3)	13.1 (10.8)	9.3 (11.8)	25.0 (6.3)	17.7 (5.9)
NZD	9.5 (5.2)	18.5 (5.9)	13.5 (15.5)	7.9 (8.7)	36.1 (6.3)	22.4 (8.1)
CAD	7.1 (7.8)	-3.6 (6.3)	-28.9 (4.7)	11.0 (9.4)	8.1 (5.0)	-17.3 (3.5)
DKK	-50.8 (47.9)	-62.5 (16.7)	-38.6 (4.4)	-30.1 (30.2)	-45.2 (10.9)	-39.4 (4.5)
CHF	-14.7 (14.3)	-28.1 (14.1)	-10.0 (3.9)	-12.8 (12.8)	-40.5 (10.2)	-14.4 (3.7)
SEK	-21.7 (21.0)	-20.5 (10.6)	-13.0 (3.5)	-7.2 (7.9)	0.4 (8.6)	-8.0 (2.5)
NOK	-25.8 (25.3)	-32.0 (17.2)	-11.7 (3.5)	-14.8 (12.3)	-19.0 (9.3)	-8.5 (2.9)
ILS	N/A (N/A)	-62.4 (65.3)	-61.1 (21.5)	N/A (N/A)	-57.0 (45.3)	-57.4 (11.0)
HKD	-4.6 (10.0)	-15.2 (10.0)	-17.8 (7.7)	-15.3 (18.0)	-5.3 (12.3)	-16.8 (6.9)
SGD	-6.9 (5.1)	-5.5 (2.8)	-1.5 (2.1)	-19.6 (15.9)	-29.8 (13.0)	-17.1 (4.8)
THB	-12.1 (13.2)	-17.0 (8.4)	-3.3 (1.7)	-9.8 (12.6)	-71.2 (41.9)	-16.8 (11.9)
MYR	-57.4 (51.7)	-74.9 (30.6)	-74.7 (19.5)	-95.2 (61.3)	-115.8 (29.9)	-77.1 (22.3)
KRW	-201.8 (115.3)	-120.3 (45.3)	-76.5 (32.8)	-114.2 (74.0)	-127.0 (43.0)	-86.0 (19.2)
RUB	62.0 (321.6)	-68.3 (33.6)	-55.4 (13.8)	117.8 (252.8)	-81.6 (36.3)	-116.3 (10.6)
ZAR	9.5 (27.9)	13.7 (15.2)	25.3 (39.3)	4.7 (26.8)	-20.8 (31.9)	-12.5 (26.5)
TRY	-120.6 (71.4)	-146.6 (62.1)	271.5 (331.7)	-115.0 (63.4)	-165.3 (39.8)	34.6 (99.8)
AED	-3.7 (20.7)	-107.2 (39.7)	-26.9 (8.4)	-6.5 (17.7)	-94.6 (33.3)	-37.0 (12.9)
SAR	-1.2 (6.5)	-50.5 (12.4)	-44.4 (11.2)	-1.6 (8.8)	-64.0 (17.1)	-64.2 (18.3)
CLP	-26.5 (60.4)	-61.8 (46.9)	-47.6 (20.2)	-12.0 (22.7)	-60.2 (16.7)	-40.6 (20.4)
MXN	-29.7 (38.5)	-103.7 (30.0)	-19.0 (19.1)	-53.0 (22.4)	-90.5 (31.5)	-26.8 (19.4)
CNY	-24.4 (67.8)	-315.3 (149.6)	-41.0 (9.4)	-36.7 (96.0)	-321.4 (125.3)	-45.0 (15.5)
QAR	N/A (N/A)	-24.4 (34.2)	25.7 (0.9)	N/A (N/A)	-36.6 (51.4)	-18.9 (0.1)

Table 2: Statistics of the CCBS in mean and standard deviations (in parentheses).N/A denotes periods for which basis observations are unavailable. ILS and QAR do not have observations during 2007–2009

obtain synthetic USD at a discount compared to the cost of direct USD in the cash market. In other words, the USD was less special compared to these currencies.

We compute daily changes in the basis by the difference in the successive daily CCBS. Table 3 reports a set of summary statistics for the daily changes in the CCBS with 1- and 5-year maturities for the full sample between January 2000 and December 2020. We report the mean (scaled by 100), standard deviation, skewness, and excess kurtosis. From the summary statistics, we notice that the daily changes on a 1-year basis have a zero mean and a relatively high standard deviation. For developed markets, the standard deviation ranges between 0.99 (New Zealand dollar - NZD) and 3.78 (Israeli shekel - ILS), while for emerging markets, it ranges between 1.40 (Thai baht - THB) and 24.26 (Russian ruble - RUB). The highest standard deviations are observed for Russia (RUB) and Turkey (TRY).

The skewness on a 1-year basis ranges from -26.67 (Israeli shekel - ILS) to 3.09 (Turkish lira - TRY), with the majority being negative. The excess kurtosis varies between 18.53 (South African rand - ZAR) and 1543.70 (Israeli shekel - ILS). Similarly, the 5-year CCBS shows a zero mean and a relatively high standard deviation. For developed markets, the standard deviation ranges between 0.62 (Swedish krona - SEK) and 2.10 (Israeli shekel - ILS), while for emerging markets it ranges between 2.48 (South African rand - ZAR) and 19.97 (Russian ruble - RUB). The second most volatile emerging-market basis after the Russian ruble (RUB) is the Chinese yuan (CNY), with a standard deviation of 10.85.

Stats	1-Year Maturity CCBS				5-Year Maturity CCBS			
	Mean	Sdev	Skew	Kurt	Mean	Sdev	Skew	Ex-Kurt
EUR	-0.10	1.91	-1.54	125.69	-0.16	0.89	-0.26	34.51
JPY	-0.29	1.63	-0.21	58.81	-0.32	1.06	0.03	46.41
GBP	0.07	1.66	-3.22	165.13	0.10	0.75	0.30	36.13
AUD	-0.14	1.19	0.92	222.55	0.03	1.08	-0.67	131.25
NZD	-0.08	0.99	0.07	38.60	0.08	0.85	0.30	37.11
CAD	-0.48	1.10	-2.07	66.13	-0.34	0.94	-22.72	1254.79
DKK	-0.47	2.22	-3.03	128.74	-0.49	1.23	-2.61	99.71
CHF	-0.15	1.68	1.08	90.50	-0.13	0.89	0.21	48.07
SEK	-0.14	1.19	-1.64	45.00	-0.06	0.62	2.42	62.27
NOK	-0.03	1.39	-6.43	395.53	-0.02	0.64	-0.33	83.54
ILS	-0.78	3.76	-26.67	1543.70	-1.03	2.10	-17.19	837.18
HKD	-0.48	1.59	0.80	29.34	-0.62	1.28	-0.91	28.00
SGD	-0.03	1.22	-0.62	126.40	-0.65	1.26	-3.87	109.29
THB	-0.07	1.40	-1.42	89.46	-0.08	2.37	-0.89	53.51
MYR	-0.90	4.91	4.59	164.20	-0.94	3.33	-0.19	26.49
KRW	-0.78	7.61	-1.93	62.05	-1.12	6.54	-1.41	28.17
RUB	-1.28	24.26	1.97	201.90	-1.78	19.97	-3.93	253.04
ZAR	1.67	3.31	0.24	18.53	0.53	2.48	0.21	30.44
TRY	-2.37	16.09	3.09	121.87	-0.06	10.24	0.44	90.87
AED	-0.38	3.29	-7.72	298.46	-0.53	3.29	-0.82	41.35
SAR	-1.01	3.64	0.33	48.64	-1.30	4.47	0.43	32.43
CLP	-0.66	4.92	-1.72	86.31	-0.32	2.29	-2.05	58.54
MXN	-0.00	4.55	1.01	93.41	0.00	2.67	-1.67	167.16
CNY	-0.56	7.71	-3.91	100.65	-0.58	10.85	-1.07	132.85
QAR	0.41	1.84	-8.11	405.74	-0.29	4.35	-2.85	166.37

Table 3: Summary statistics of daily changes in cross-currency basis swaps (Jan 2000–December 2020).

The skewness of the daily changes in the 5-year CCBS ranges from -22.72 (Canadian dollar - CAD) to 2.42 (Swedish krona - SEK), with the majority being negative. The excess kurtosis varies between 26.49 (Malaysian ringgit - MYR) and 1254.79 (Canadian dollar - CAD). Overall, the daily changes in both the 1- and 5-year CCBS show a leptokurtic behaviour, characterised by high peaks and fat tails compared to a normal distribution.

5. Empirical Findings and Discussion

This section presents the empirical analysis of cross-currency basis swap (CCBS) interconnectedness using the BGSVAR framework introduced earlier. The analysis evaluates the model's testable propositions and addresses the research questions posed in the Introduction: (i) whether movements in CCBS spreads reflect systemic contagion, and (ii) which currencies occupy central positions in transmitting funding shocks across the network.

5.1. Rolling BGSVAR Specification and Lag Selection

We analyse the interconnectedness among the G-25 CCBS using a rolling one-year window of approximately 240 trading days. The window is advanced in monthly increments, beginning with February 2000-January 2001 and ending with July 2019-December 2020, resulting in a total of 234 estimation windows.

Because CCBS data are not uniformly available across currencies in the early part of the sample, the effective cross-section varies over time. For each window, we include only currencies with complete observations. This approach ensures that all estimations are based on fully observed data, thereby avoiding biases from interpolation or missing-data imputation. As a result, each estimated network reflects contemporaneous market conditions, and changes in topology capture genuine structural evolution rather than artefacts of data construction.

p	1	2	3	4	5	6	7
BIC (1Y)	**48.15**	48.27	48.58	48.96	49.30	49.65	50.10
BIC (5Y)	**35.79**	36.25	36.75	37.30	37.89	38.51	39.11

Table 4: The BIC for lag order selection. Boldface values indicate the minimum BIC.

The optimal lag order for the BGSVAR is selected using the Bayesian Information Criterion (BIC) over $p \in \{1, \dots, 7\}$. Table 4 reports the results. For both maturities, the BIC is minimised at $p = 1$, which we adopt throughout.

5.2. Network Density and Financial Turbulence

We now address Research Question 1 (RQ-1): *Do movements in cross-currency basis swap spreads reflect systemic contagion rather than isolated fluctuations*?

To do so, we examine the network density and a turbulence index introduced in Section 3. Figure 3 plots these metrics for 1-year and 5-year maturities. Their time-varying behaviour reveals four distinct phases in the evolution of market stress.

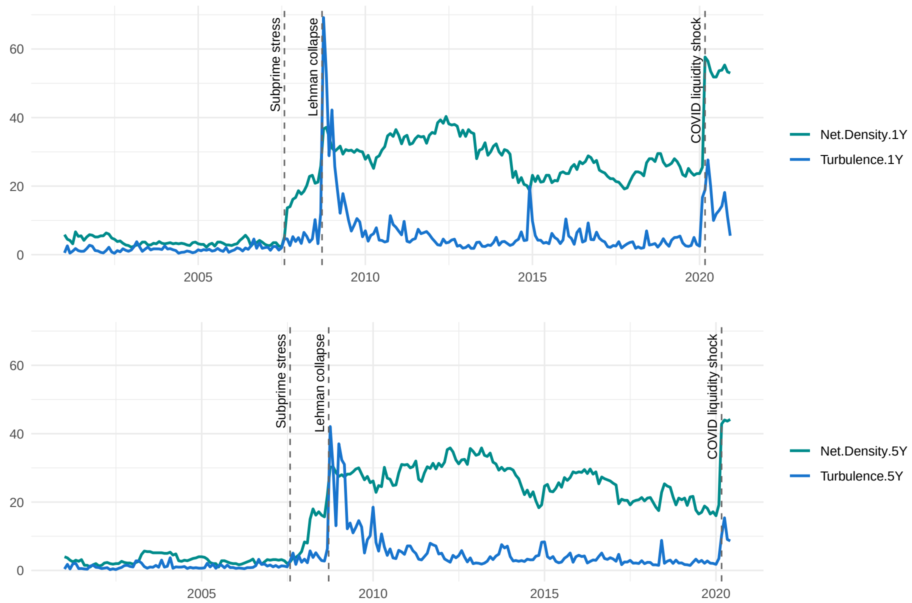

Figure 3: Network Density and Turbulence Index among CCBS with **1 & 5-year** maturities. The green line denotes network density, while the blue line denotes turbulence index. Results are shown for the 1-year (top panel) and 5-year (bottom panel) maturities. Vertical dashed lines denote key financial events: the onset of subprime stress (August 2007), the Lehman Brothers collapse (September 2008), and the COVID-19 USD liquidity shock (March 2020).

Pre-crisis period (2000–2006): This period is characterised by low network density and subdued turbulence, indicating weak cross-currency spillovers and a stable funding environment. This is consistent with near-zero CIP deviations documented in the pre-2007 literature.

Global Financial Crisis - GFC (2007–2009): The network density rises sharply, signalling the onset of systemic contagion, while turbulence spikes to its highest level in the sample, marking a severe market dislocation. This pattern is consistent with the model's contagion amplification mechanism, whereby increases in Λ_t induce near-rank-one comovement.

Eurozone sovereign crisis (2010–2013). Network density remains elevated, albeit below GFC peaks, while turbulence exhibits episodic surges reflecting region-specific funding stress.

Recent period (2014–2020). Network density trends upward, indicating deeper integration and greater interdependence in the CCBS market. The COVID-19 shock generates a spike in turbulence, albeit smaller than during the GFC. Notably, network density during this episode exceeds GFC levels, suggesting a broader diffusion of stress despite lower aggregate volatility.

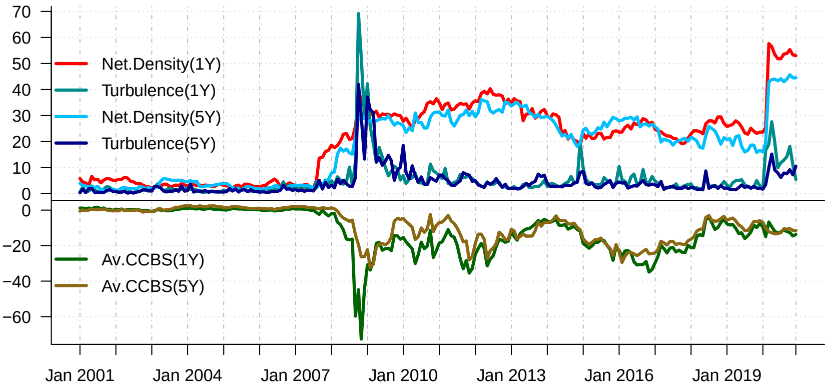

Figure 4: Network Density, Turbulence Index and Average Cross-Currency Basis Swap Spread of G-10. from January 2001 to December 2020.

x_{t+h}	-4	-3	-2	-1	0	1	2	3	4
	Cross Correlation of ΔNet.Density (1Y) with								
Δ Av.CCBS (1Y)	0.023	-0.020	0.065	0.066	**-0.312**	-0.008	0.030	0.053	0.033
	Cross Correlation of ΔTurbulence (1Y) with								
Δ Av.CCBS (1Y)	-0.011	0.129	-0.067	0.131	**-0.315**	-0.302	0.105	0.137	0.024
	Cross Correlation of ΔTurbulence (1Y) with								
ΔNet.Density (1Y)	0.036	-0.200	-0.054	0.062	**0.318**	0.048	-0.090	0.027	-0.035
	Cross Correlation of ΔNet.Density (5Y) with								
Δ Av.CCBS (5Y)	-0.079	-0.058	-0.017	0.125	-0.109	**-0.189**	-0.150	-0.005	0.014
	Cross Correlation of ΔTurbulence (5Y) with								
Δ Av.CCBS (5Y)	0.021	0.025	0.066	-0.068	0.120	**-0.425**	0.124	-0.084	0.035
	Cross Correlation of ΔTurbulence (5Y) with								
ΔNet.Density (5Y)	-0.079	-0.007	-0.086	0.016	**0.254**	0.012	-0.046	0.013	0.011

Table 5: Cross-correlation between the average basis, network density, and the turbulence index for both maturities. Entries report correlations between x_{t+h} (row variable) and y_t (column variable). Boldface values denote statistical significance.

These patterns indicate that modern CCBS markets are increasingly interconnected, even during episodes characterised by moderate levels of aggregate stress.

5.2.1. Disentangling Common Funding Shocks from Cross-Currency Dependence

An identification concern is whether the estimated network reflects genuine cross-currency dependence or merely shared exposure to global USD funding conditions. In the theoretical framework, both bilateral linkages (Φ) and a global funding factor (Λ_t) generate co-movement across basis spreads. As a result, elevated connectedness during crisis periods could arise even in the absence of cross-currency transmission.

To address this, we purge each series of a proxy for global funding conditions and re-estimate the network. Specifically, within each rolling window, we regress each currency's basis change on the cross-sectional average of G10 currencies' basis changes and use the resulting residuals to construct the network. This procedure removes the component of basis variation driven by common global shocks while preserving idiosyncratic and cross-currency dynamics.

Figure 5 presents network density alongside the baseline measure for both the 1-year and 5-year maturities. In both cases, the two series are nearly indistinguishable over the full sample. In particular, the pronounced increase in connectedness during the Global Financial Crisis and the COVID-19 episode remains intact after purging the common factor.

Figure 5: Network density before and after purging a global funding factor. The red line denotes baseline density, while the green line denotes density computed using factor-purged residuals. Results are shown for the 1-year (top panel) and 5-year (bottom panel) maturities. Vertical dashed lines denote key financial events: the onset of subprime stress (August 2007), the Lehman Brothers collapse (September 2008), and the COVID-19 USD liquidity shock (March 2020).

This result indicates that the estimated network structure is not primarily driven by shared exposure to global USD funding stress. Instead, the persistence of elevated density after removing the common component suggests that the network captures robust conditional dependence across currencies. While global funding conditions (Λ_t) clearly contribute to co-movement in basis spreads, they do not fully account for the observed interconnectedness.

Taken together, these findings provide strong support for the interpretation that CCBS markets behave as an interconnected system in which movements in individual currencies are linked through cross-currency dynamics, rather than merely reflecting a common global shock.

5.2.2. Interpreting Interconnectedness: Funding Conditions and Demand for USD

Having established that the network structure is not driven solely by a common global factor, we now turn to its economic interpretation. While our theoretical framework highlights the role of tighter dealer balance-sheet constraints and global funding tightness (Λ_t), the observed rise in interconnectedness during crisis episodes is also consistent with simultaneous increases in global demand for USD funding and hedging.

Because the empirical analysis identifies equilibrium outcomes in cross-currency basis spreads, it does not separately recover supply and demand schedules. As a result, the observed co-movement reflects the combined effects of these forces. Periods of stress are characterised by higher marginal costs of intermediation and stronger demand for hedged USD funding, which together contribute to wider basis spreads and stronger network linkages.

To further assess the relationship between market stress and interconnectedness, Figure 4 plots the average G-10 basis spreads alongside network density and turbulence. During all major stress episodes, large declines in the cross-currency basis coincide with increases in both density and turbulence. This behaviour is consistent with the model's predictions and reflects the joint role of global funding conditions and synchronised demand for USD liquidity.

This relationship is further supported by the cross-correlation analysis in Table 5. For the 1-year maturity, the strongest correlation with the basis occurs contemporaneously (lag 0), while for the 5-year maturity it peaks at lag 1, consistent with the Maturity Heterogeneity proposition.

Both network density and turbulence display a positive contemporaneous correlation, indicating that periods of higher interconnectedness are typically associated with heightened volatility and rapid adjustments in market structure.

Based on the similarity in the dynamics of network density and the turbulence index, two stylised facts emerge:

First, *the COVID-19 episode resembles the GFC in structural terms.* Although the turbulence spike during COVID-19 was smaller than during the GFC, the degree of interconnectedness was substantially higher. This reflects the larger global dealer footprint, broader cross-currency balance-sheet linkages (Φ), and the faster transmission of USD funding shocks in modern markets. Consistent with Proposition 1, increases in global funding tightness (Λ_t) push the system toward a near rank-one structure, generating highly synchronised movements in the basis. Empirically, this is exactly what we observe during both crises.

Second, *the post-pandemic adjustment mirrors the post-GFC normalisation.* The steady decline in network density and turbulence after 2020 signals a transition toward a more tranquil regime marked by reduced market stress, lower USD funding pressure, and less negative CIP deviations. In line with Avdjiev et al. (2019a), episodes of USD weakness are typically accompanied by stronger cross-border banking flows, improved offshore USD liquidity, and tighter basis spreads. Together, these developments suggest that the CCBS market is reverting to a more stable configuration, echoing the post-GFC normalisation path.

In summary, across maturities and market regimes, the evidence shows that large negative CIP deviations coincide with elevated connectedness and heightened turbulence, and that the CCBS system behaves as a tightly linked network during periods of stress. These patterns are fully consistent with the model's predictions on contagion amplification and maturity heterogeneity. Overall, the findings provide strong evidence that movements in cross-currency basis swap spreads reflect systemic contagion rather than isolated currency-specific shocks. The evidence is consistent with a framework in which dealer balance-sheet constraints and synchronised global demand for USD funding jointly contribute to heightened interconnectedness during crisis episodes.

These findings are broadly consistent with prior evidence showing that CIP deviations intensify during episodes of systemic stress and global USD funding shortages (Baba and Packer, 2009a; Du et al., 2018; Avdjiev et al., 2019a). However, whereas much of the existing literature focuses primarily on bilateral deviations or aggregate funding conditions, our results extend this evidence by demonstrating that modern CCBS markets behave as densely interconnected networks in which stress propagates simultaneously across currencies. The sharp increase in network density and turbulence during crisis periods supports the view that system-wide contagion, rather than isolated currency-specific dislocations, characterises modern CCBS markets. These patterns are consistent with a framework in which dealer balance-sheet constraints, global funding tightness, and synchronised demand for USD funding jointly contribute to the propagation of stress across currencies.

5.3. Network Topology and Centrality

We now turn to the second research question (RQ-2): *In the event of contagion, which basis swap spreads are most central in propagating spillovers across the foreign exchange derivatives market?*

To address this question, we examine the dynamic topological structure of the G-25 CCBS network and compute standard centrality measures to identify the currencies that act as key transmitters of shocks. From our estimated networks, we compute hub and authority scores to characterise the directional importance of each currency. Hub scores summarise the extent to which a currency sends shocks to others, while authority scores capture the extent to which it receives shocks. These measures provide an empirical analogue to the theoretical centrality metric $C_k = \sum_{j \neq k} \phi_{kj}$ introduced earlier.

Figure 6 and 7 display the estimated networks for six sub-periods: 2001–2006, 2007–2009, 2010–2013, 2014–2016, 2017–2019, and 2020, for both 1-year and 5-year maturities. Links are colour-coded by sign (red for negative effects and green for positive), while node colours distinguish developed (red) and emerging (blue) markets. Node sizes are proportional to hub scores, allowing for a direct visual assessment of currency importance.

Several patterns emerge. First, there is clear evidence of clustering behaviour: developed market currencies tend to form one cluster and emerging markets another, reflecting similarities in funding structures and regulatory environments. Second, although the early sample (2001–2006) shows some dispersion, with NOK and DKK appearing as the most influential nodes, the post-2007 networks consistently place the Euro (EUR) at the centre of the system. This is especially pronounced during the GFC (2007–2009) and the Eurozone crisis (2010–2013), where EUR plays a dominant role in transmitting shocks to other currencies. In contrast, peripheral emerging market currencies tend to have low degrees of influence and largely absorb shocks rather than propagate them.

Table 6 displays the hub and authority rankings across sub-periods for both maturities, organised into "core", "semi-periphery", and "periphery" groups. For the 1-year maturity, EUR, DKK, CHF, JPY, and ZAR dominate the hub ranking; for the 5-year maturity, EUR, CHF, JPY, DKK, and SEK appear as the most influential. Authority rankings highlight JPY,

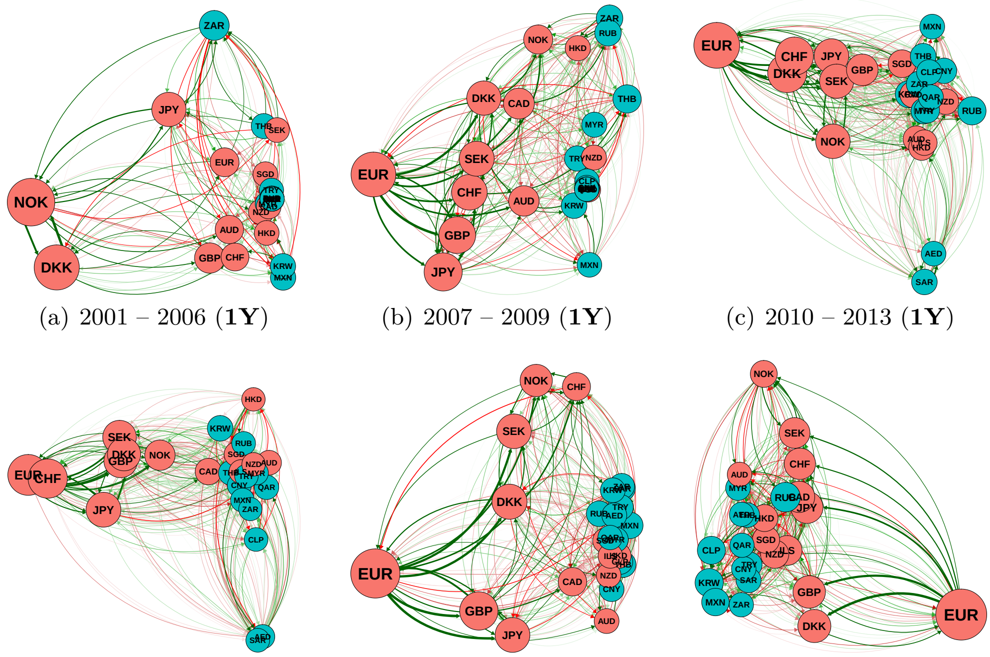

(a) 2001 – 2006 (**1Y**) (b) 2007 – 2009 (**1Y**) (c) 2010 – 2013 (**1Y**)

(d) 2014 – 2016 (**1Y**) (e) 2017 – 2019 (**1Y**) (f) 2020 (**1Y**)

Figure 6: Networks of CCBS with **1-year** maturity. Red links denote negative effects and green for positive interactions. Red (blue) nodes are developed (emerging) market currencies.

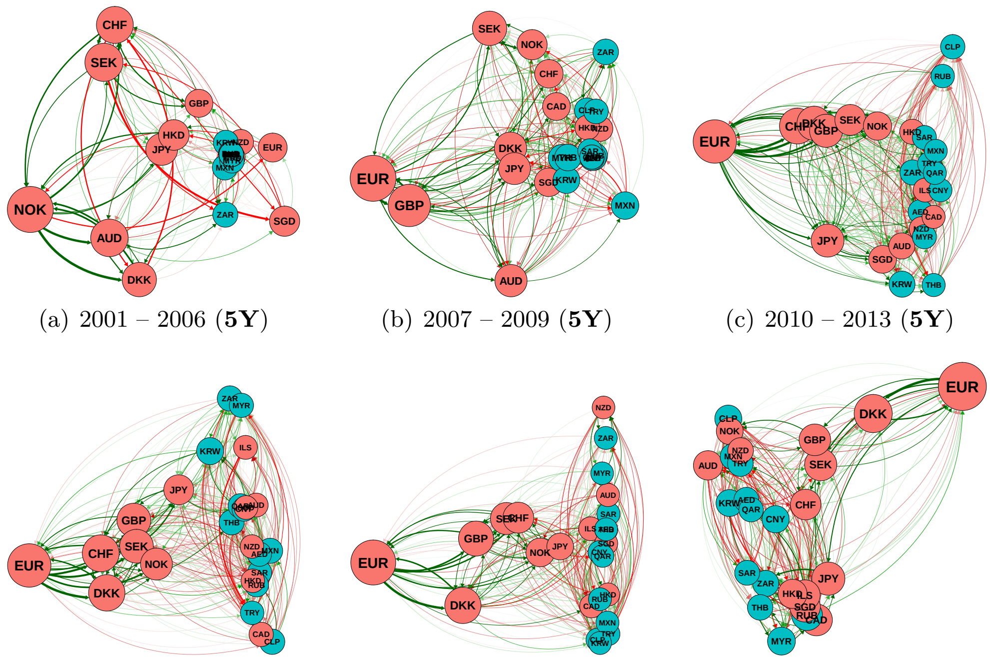

(a) 2001 – 2006 (**5Y**) (b) 2007 – 2009 (**5Y**) (c) 2010 – 2013 (**5Y**)

(d) 2014 – 2016 (**5Y**) (e) 2017 – 2019 (**5Y**) (f) 2020 (**5Y**)

Figure 7: Networks of CCBS with **5-year** maturity. Red links denote negative effects and green for positive interactions. Red (blue) nodes are developed (emerging) market currencies.

	Rank	1-Year Maturity CCBS		5-Year Maturity CCBS	
		Hub	Auth	Hub	Auth
Sub-Periods: Top Three Most Influential Currencies					
2001 – 2006	1	ZAR (0.423)	JPY (0.267)	SEK (0.243)	NOK (0.243)
	2	HKD (0.291)	KRW (0.244)	HKD (0.219)	AUD (0.200)
	3	NOK (0.264)	ZAR (0.239)	AUD (0.176)	ZAR (0.181)
2007 – 2009	1	JPY (0.291)	JPY (0.274)	JPY (0.279)	JPY (0.277)
	2	EUR (0.286)	DKK (0.253)	CAD (0.242)	DKK (0.269)
	3	DKK (0.251)	MXN (0.247)	GBP (0.238)	SGD (0.258)
2010 – 2013	1	EUR (0.269)	SEK (0.272)	EUR (0.277)	EUR (0.297)
	2	CHF (0.256)	EUR (0.255)	SEK (0.266)	JPY (0.254)
	3	SEK (0.255)	JPY (0.251)	JPY (0.225)	CHF (0.237)
2014 – 2016	1	CHF (0.282)	JPY (0.273)	EUR (0.252)	KRW (0.251)
	2	JPY (0.249)	CLP (0.248)	ZAR (0.249)	EUR (0.249)
	3	EUR (0.232)	SEK (0.218)	CNY (0.245)	RUB (0.238)
2017 – 2019	1	EUR (0.304)	EUR (0.306)	EUR (0.293)	DKK (0.277)
	2	DKK (0.299)	CHF (0.295)	DKK (0.268)	GBP (0.257)
	3	CHF (0.260)	DKK (0.282)	GBP (0.264)	EUR (0.243)
2020	1	KRW (0.247)	JPY (0.262)	KRW (0.315)	ZAR (0.267)
	2	EUR (0.245)	KRW (0.251)	JPY (0.273)	TRY (0.253)
	3	GBP (0.239)	NOK (0.248)	AUD (0.270)	JPY (0.252)
Full-Sample: All G-25 Currencies					
Core	1	EUR (0.253)	JPY (0.260)	EUR (0.229)	JPY (0.223)
	2	DKK (0.243)	NOK (0.238)	CHF (0.219)	EUR (0.221)
	3	CHF (0.239)	SEK (0.227)	JPY (0.211)	CHF (0.218)
	4	JPY (0.227)	DKK (0.220)	DKK (0.197)	KRW (0.216)
	5	ZAR (0.220)	EUR (0.219)	SEK (0.192)	GBP (0.212)
Semi-Periphery	6	NOK (0.216)	KRW (0.216)	KRW (0.190)	ZAR (0.203)
	7	SEK (0.210)	GBP (0.213)	ZAR (0.189)	DKK (0.193)
	8	GBP (0.207)	CHF (0.204)	MYR (0.184)	SEK (0.171)
	9	HKD (0.192)	ZAR (0.188)	GBP (0.171)	NOK (0.169)
	10	MXN (0.187)	HKD (0.176)	HKD (0.169)	HKD (0.157)
	11	KRW (0.178)	MXN (0.167)	AUD (0.164)	MYR (0.157)
	12	RUB (0.169)	RUB (0.155)	RUB (0.154)	RUB (0.155)
	13	MYR (0.154)	AUD (0.151)	THB (0.148)	THB (0.151)
	14	THB (0.128)	CAD (0.148)	MXN (0.130)	MXN (0.150)
	15	CAD (0.124)	MYR (0.144)	NOK (0.121)	CLP (0.145)
Periphery	16	AUD (0.123)	THB (0.126)	TRY (0.121)	SGD (0.142)
	17	TRY (0.114)	NZD (0.117)	CLP (0.121)	AUD (0.137)
	18	SGD (0.104)	TRY (0.113)	SGD (0.120)	TRY (0.131)
	19	SAR (0.103)	CNY (0.096)	SAR (0.115)	AED (0.114)
	20	NZD (0.101)	SGD (0.078)	NZD (0.093)	CAD (0.106)
	21	CLP (0.071)	SAR (0.077)	CAD (0.092)	NZD (0.099)
	22	CNY (0.071)	AED (0.051)	AED (0.084)	SAR (0.090)
	23	AED (0.049)	CLP (0.044)	CNY (0.075)	CNY (0.067)
	24	ILS (0.000)	ILS (0.000)	ILS (0.000)	ILS (0.000)
	25	QAR (0.000)	QAR (0.000)	QAR (0.000)	QAR (0.000)

Table 6: Centrality ranking 1-year and 5-year swaps of according to hub and authority score.

EUR, CHF, and DKK as the main receivers of shocks. Notably, KRW and ZAR emerge as non-European currencies with elevated centrality, particularly at the short end.

The persistent dominance of the euro across maturities and subperiods likely reflects the central role of the euro area as the largest non-USD funding system and the extensive balance-sheet linkages maintained by major European dealer banks. In addition, many euro-area institutional investors and asset managers operate under currency-hedged return mandates, which require them to hedge a substantial fraction of their dollar-denominated exposures. These structural features generate large and persistent hedging flows and reinforce the euro's position as a key transmitter of funding shocks within the global cross-currency basis network. The euro's prominence may also reflect a substitution mechanism in synthetic dollar funding markets. Because the EUR–USD swap market is among the deepest and most liquid channels for obtaining synthetic dollars, borrowers and investors often rely on the euro as a primary funding conduit. As demand for synthetic dollars rises and dealer balance-sheet capacity becomes increasingly constrained, the EUR–USD basis widens and the cost of obtaining dollars through euro swaps increases. Market participants may then increasingly seek alternative funding channels where synthetic dollar funding remains relatively cheaper. As these channels become more heavily utilised, pressures may propagate across currencies and basis spreads widen more broadly. In this sense, the euro may act not only as the largest node in the network, but also as an important conduit through which widening pressures are transmitted to the wider system. The emergence of KRW and ZAR as relatively central non-European currencies, particularly during the COVID-19 episode, suggests that the geography of offshore dollar funding has become increasingly global. Their elevated centrality indicates that stress propagation is no longer confined to the traditional European core but increasingly reflects the growing importance of Asian and commodity-related funding channels. More broadly, these findings are consistent with a gradual expansion of the offshore dollar funding system beyond its historical European centres and with an increasing diversification of synthetic dollar funding routes outside the traditional European core.

Collectively, these results indicate that the most critical currencies for shock propagation are the *Euro (EUR)*, *Swiss franc (CHF)*, and *Danish krone (DKK)*, followed by *Japanese yen (JPY)*. This finding is economically intuitive and consistent with our theoretical framework. EUR, CHF, and DKK lie at the core of the European banking system, which plays a central role in global USD funding markets. European financial institutions often obtain USD through FX swaps using Euro- and Swiss franc-denominated liabilities, generating strong cross-currency balance-sheet linkages. As a consequence, stresses in these currencies' basis propagate disproportionately across the entire network. The dominance of JPY in authority rankings reflects the structural role of Japanese banks in global USD intermediation.

Overall, the topology of the network shows that spillover propagation is *Euro-centred.* Shocks that disrupt the functioning of global USD funding markets tend to manifest first in the Euro basis before spreading to others. The liquidity and market depth of the EUR-USD pair reinforce this outcome, as the Euro basis remains the most actively traded cross-currency basis in global derivative markets.

Consistent with this result, the Euro-centred structure of cross-currency basis interconnectedness can be understood through the lens of global funding demand and dealer balance-sheet intermediation. The Euro is the largest non-U.S. currency used in international bond issuance and serves as an important funding currency for global investors. A substantial fraction of Euro-denominated issuance is not held in Euros, but instead swapped into USD through the cross-currency swap market. This allows institutions with Euro-denominated liabilities to obtain USD funding via swaps while also hedging exchange rate risk. As demand for synthetic USD through FX swaps increases, intermediaries supplying this intermediation face rising balance-sheet costs. These costs arise from regulatory capital constraints, internal risk limits, and the opportunity cost of scarce balance-sheet capacity. In equilibrium, intermediaries supply synthetic USD up to the point where the marginal benefit equals the marginal balance-sheet cost. As this marginal cost rises, the CIP deviation widens, increasing the cost of obtaining synthetic USD funding through the swap market.

Because Euro-based funding flows are large and central to global markets, they place significant pressure on dealer balance sheets. In our framework, this corresponds to strong cross-currency linkages captured by the matrix Φ, which reflects the fact that intermediation in one currency pair consumes balance-sheet capacity that is shared across markets. As a result, shocks that increase the cost of intermediating Euro–USD swaps raise the marginal cost of supplying synthetic USD in other currencies, generating spillovers across the network of basis spreads. This mechanism also explains the centrality of the Swiss franc and Danish krone. The Danish krone is tightly linked to the Euro through its exchange-rate arrangement, while the Swiss franc is deeply integrated into European financial markets and frequently used as a funding currency. As a result, USD funding demand in these currencies is closely tied to Euro-area funding conditions. When Euro-related funding pressures intensify, demand for hedged USD funding via swaps rises not only for Euro-based borrowers but also for institutions operating in closely linked currencies such as CHF and DKK. Importantly, institutions rely on FX swaps rather than direct USD borrowing because swaps allow them to hedge currency risk while accessing USD funding. Unhedged borrowing would expose balance sheets to exchange rate fluctuations, particularly for institutions with non-USD liabilities. The swap market, therefore, becomes the primary channel through which global USD funding demand is intermediated, even when it becomes more costly.

Collectively, these forces imply that the Euro, Swiss franc, and Danish krone occupy central positions in the global FX funding network. Their associated basis spreads reflect the marginal cost of USD intermediation in core funding markets, and shocks to these markets propagate broadly through shared dealer balance sheets. This explains why widening in Euro-related basis spreads transmits to other currencies and why the network of CIP deviations exhibits a strongly Euro-centred structure.

Our centrality results also complement and extend the broader literature on offshore USD funding markets and intermediary balance-sheet constraints. Previous studies emphasise the importance of global USD funding conditions in shaping CIP deviations. Our findings contribute to this literature by showing that spillover transmission is not uniformly distributed across currencies, but instead concentrated around a small set of structurally central funding currencies, particularly the Euro. This suggests that the topology of the dealer-intermediation network plays an important role in determining how funding shocks propagate internationally.

6. Conclusion

6.1. Main Findings

This paper examined whether cross-currency basis swap (CCBS) spreads reflect systemic contagion and which currencies occupy central positions in transmitting funding shocks through global offshore USD funding markets. Using a Bayesian graphical structural VAR (BGSVAR) framework, we recover a sparse and directed network of spillovers that characterises how shocks to funding conditions propagate across currencies over time.

First, our findings show that movements in CCBS spreads reflect systemic contagion rather than isolated currency-specific dislocations. Network density and turbulence rise sharply during periods of financial stress, particularly during the Global Financial Crisis and the COVID-19 pandemic, indicating that global USD funding tightness generates highly synchronised spillovers across currencies. During these episodes, the system compresses toward a near rank-one structure, implying that a common global funding factor dominates basis dynamics. These findings strongly support the Contagion Amplification proposition developed in the theoretical framework.

Second, our analysis shows that spillover transmission is highly concentrated around a relatively small number of structurally central currencies. In particular, the Euro consistently emerges as the dominant hub currency, with the Swiss franc and Danish krone also occupying systemically important positions in the dealer-intermediation network. These results support the model's Currency Centrality proposition and indicate that offshore USD funding stress propagates through a highly asymmetric network structure centred around European funding markets.

Third, we document substantial heterogeneity across maturities and exchange-rate regimes. Short-tenor basis spreads exhibit stronger contagion and greater volatility than long-tenor spreads, while currencies with tighter exchange-rate pegs to the USD display comparatively muted spillover dynamics during crisis periods. These findings are consistent with the model's predictions regarding maturity heterogeneity and pegged-currency insulation, and suggest that both market structure and exchange-rate arrangements influence the transmission of global funding shocks.

Taken together, the theoretical and empirical results point to a common mechanism: deviations from covered interest parity arise as equilibrium outcomes of constrained global USD intermediation, with their magnitude and propagation governed by dealer balance-sheet frictions and network structure.

6.2. Implications for Market Participants and Policymakers

The findings of this paper carry several practical implications for market participants and policymakers operating in environments characterised by persistent deviations from covered interest parity and elevated global USD funding stress.

First, the evidence that contagion intensifies sharply during crisis periods implies that hedging costs and synthetic USD funding conditions can become highly synchronised across currencies during episodes of systemic stress. In particular, our finding that short-tenor basis spreads exhibit stronger contagion and higher volatility suggests that short-maturity hedging strategies may be especially vulnerable to sudden funding dislocations. For institutions managing foreign exchange exposures, movements in the EUR–USD basis therefore provide important information about broader conditions in global USD funding markets.

Second, the dominant centrality of the Euro basis implies that European funding conditions play a disproportionately important role in transmitting shocks across the global CCBS network. Because EUR, CHF, and DKK occupy the most central positions in the network, disruptions affecting European dealer balance sheets can generate system-wide spillovers across offshore USD funding markets. Monitoring movements in the Euro basis may therefore help policymakers and market participants identify periods of tightening dealer balance-sheet conditions and rising systemic funding stress.

Third, our findings suggest that persistent CIP deviations primarily reflect intermediary balance-sheet constraints and global funding frictions rather than temporary arbitrage mispricing. As a result, policy interventions that relax dealer funding pressures, such as central bank swap lines and emergency liquidity facilities, can play an important stabilising role by reducing the marginal cost of USD intermediation and dampening the cross-currency propagation of shocks. Within our theoretical framework, such interventions operate by weakening the transmission channel embedded in the dealer-intermediation network.

More broadly, the results suggest that global funding markets are best understood as an interconnected system in which local disruptions can generate large and nonlinear spillovers through shared intermediary balance sheets. This perspective has implications not only for CIP deviations, but also for the international transmission of monetary policy, global liquidity conditions, and the resilience of the international financial system more generally.

6.3. Study Limitations and Future Research

Several limitations of the present study suggest directions for future research. First, although the BGSVAR framework effectively captures dynamic spillover networks, it remains a reduced-form representation and therefore does not fully identify the underlying structural mechanisms governing dealer balance-sheet adjustment and liquidity provision. Future research could incorporate institution-level balance-sheet data, dealer-specific exposures, or transaction-level funding information to better identify the microeconomic channels underlying CCBS interconnectedness.

Second, while our analysis spans a broad cross-section of developed and emerging-market currencies, data limitations constrain the availability of certain currencies and maturities during the earlier part of the sample. Future work could examine more granular tenor structures, higher-frequency funding dynamics, or post-2020 developments associated with changing monetary-policy regimes and geopolitical fragmentation.

Moreover, the present framework treats currencies symmetrically and may understate the hierarchical structure of funding markets in emerging economies. Examining EME subnetworks and the intermediary role of regional hub currencies represents a promising avenue for future research.

Finally, our framework focuses primarily on spillover transmission through offshore USD funding markets. Future research could explore how CCBS interconnectedness interacts with broader macro-financial variables such as global capital flows, sovereign risk, banking-sector fragility, and central-bank liquidity interventions.

An important qualification is that the empirical analysis does not separately identify supply-side and demand-side sources of funding stress. Although the theoretical framework emphasises intermediary balance-sheet constraints, the evidence is equally consistent with episodes in which synchronised demand for USD funding and hedging amplifies cross-currency comovement. Future research may seek to disentangle these channels more explicitly.

In sum, this paper shows that deviations from covered interest parity are not isolated anomalies but are instead manifestations of a tightly interconnected global funding system in which the cost and availability of USD liquidity are jointly determined by constrained intermediaries operating across a network of currencies. Understanding this structure is essential for interpreting market dynamics, designing effective policy interventions, and managing risk in an increasingly interconnected international financial system.

Declaration

Availability of Data: The data that supports the findings of this study is available from the corresponding author upon reasonable request.

References

Abakah, E. J. A., M. Brahim, J.-E. Carlotti, A. K. Tiwari, and W. Mensi (2024). Extreme Downside Risk Connectedness and Portfolio Hedging Among the G10 Currencies. *International Economics 178*, 1–26.

Ahelegbey, D. F., M. Billio, and R. Casarin (2016). Bayesian Graphical Models for Structural Vector Autoregressive Processes. *Journal of Applied Econometrics 31*(2), 357–386.

Ahelegbey, D. F. and P. Giudici (2022). NetVIX - A Network Volatility Index of Financial Markets. *Physica A: Statistical Mechanics and its Applications 594*, 127017.

Aizenman, J., H. Ito, and G. K. Pasricha (2022). Central Bank Swap Arrangements in the COVID-19 Crisis. *Journal of International Money and Finance 122*, 1–20.

Aizenman, J. and G. K. Pasricha (2010). Selective Swap Arrangements and the Global Financial Crisis: Analysis and Interpretation. *International Review of Economics & Finance 19*(3), 353–365.

Avdjiev, S., W. Du, C. Koch, and H. S. Shin (2019a). The Dollar, Bank Leverage, and Deviations from Covered Interest Parity. *American Economic Review: Insights 1*(2), 193–208.

Avdjiev, S., E. Eren, and P. McGuire (2020). Dollar Funding Costs During the Covid-19 Crisis Through the Lens of the FX Swap Market. Technical report, Bank for International Settlements.

Avdjiev, S., P. Giudici, and A. Spelta (2019b). Measuring Contagion Risk In International Banking. *Journal of Financial Stability 42*, 36–51.

Baba, N. and F. Packer (2009a). From Turmoil to Crisis: Dislocations in the FX Swap Market Before and After the Failure of Lehman Brothers. *Journal of International Money and Finance 28*(8), 1350–1374.

Baba, N. and F. Packer (2009b). Interpreting Deviations from Covered Interest Parity During the Financial Market Turmoil of 2007–08. *Journal of Banking and Finance 33*(11), 1953–1962.

Baba, N., F. Packer, and T. Nagano (2008). The Spillover of Money Market Turbulence to FX Swap and Cross-Currency Swap Markets. *BIS Quarterly Review March*, 73–86.

Ben Zeev, N. and D. Nathan (2024). The Widening of Cross-currency Basis: When Increased FX Swap Demand Meets Limits of Arbitrage. *Journal of International Economics 152*, 103984.

Borio, C. E., R. N. McCauley, P. McGuire, and V. Sushko (2016). Covered Interest Parity Lost: Understanding the Cross-Currency Basis. Technical report, BIS Quarterly Review.

Callier, P. (1981). One Way Arbitrage, Foreign Exchange and Securities Markets: A Note. *The Journal of Finance 36*(5), 1177–1186.

Cerutti, E., M. Obstfeld, and H. Zhou (2021). Covered Interest Parity Deviations: Macrofinancial Determinants. *Journal of International Economics 130*, 1–24.

Cerutti, E. and H. Zhou (2024). Uncovering CIP Deviations in Emerging Markets: Distinctions, Determinants, and Disconnect. *IMF Economic Review 72*, 196–252.

Coffey, N., W. B. Hrung, and A. Sarkar (2009). Capital Constraints, Counterparty Risk, and Deviations from Covered Interest Rate Parity. Staff reports, Federal Reserve Bank of New York.

Cunado, J., D. Gabauer, R. Gupta, and C.-C. Lee (2024). On the Propagation Mechanism of International Real Interest Rate Spillovers: Evidence from More than 200 Years of Data. *Applied Economics 1*, 1–15.

Du, W. and J. Schreger (2016). Local Currency Sovereign Risk. *The Journal of Finance 71*(3), 1027–1070.

Du, W., A. Tepper, and A. Verdelhan (2018). Deviations from Covered Interest Rate Parity. *The Journal of Finance 73*(3), 915–957.

Duffie, D. (2010). The Failure Mechanics of Dealer Banks. *Journal of Economic Perspectives 24*(1), 51–72.

Eguren-Martin, F., M. O. Busch, and D. Reinhardt (2024). Global Banks and Synthetic Funding: The Benefits of Foreign Relatives. *Journal of Money, Credit and Banking 56*(6), 115–152.

Fong, W.-M., G. Valente, and J. K. Fung (2010). Covered Interest Arbitrage Profits: The Role of Liquidity and Credit Risk. *Journal of Banking and Finance 34*(5), 1098–1107.

Garleanu, N. and L. H. Pedersen (2011). Margin-based Asset Pricing and Deviations from the Law of One Price. *The Review of Financial Studies 24*(6), 1980–2022.

Geyikci, U. B. and S. Özyildirim (2023). Deviations from Covered Interest Parity in the Emerging Markets After the Global Financial Crisis. *Journal of International Financial Markets, Institutions and Money 85*, 1–18.

He, Z. and A. Krishnamurthy (2013). Intermediary Asset Pricing. *American Economic Review 103*(2), 732–770.

Hui, C.-H., H. Genberg, and T.-K. Chung (2011). Funding Liquidity Risk and Deviations from Interest-Rate Parity During the Financial Crisis of 2007-2009. *International Journal of Finance and Economics 16*(4), 307–323.

Ibhagui, O. (2019). Interrelations among Cross-Currency Basis Swap Spreads: Pre-and Post-crisis Analysis. *The Journal of Derivatives 26*(4), 89–112.

Shleifer, A. and R. W. Vishny (1997). The Limits of Arbitrage. *The Journal of Finance 52*(1), 35–55.

Stenfors, A., I. Chatziantoniou, and D. Gabauer (2022). Independent Policy, Dependent Out-comes: A Game of Cross-Country Dominoes across European Yield Curves. *Journal of International Financial Markets, Institutions and Money 81*, 1–21.

A. Proofs of the Propositions

We provide the formal proofs of the propositions stated in Section 2. To ensure that the model is well-posed and that the propositions hold, we impose the following assumptions.

Assumption 1 (Positivity and boundedness)**.** *T is diagonal with $\tau_k \geq 0$, Φ is symmetric with $\phi_{ij} \geq 0$, and both T and Φ are time-invariant. There exist constants $0 < m \leq M < \infty$ such that*

$$mI \preceq T + \Phi \preceq MI.$$

Hence $T + \Phi$ is positive definite and well-conditioned.

Assumption 2 (Demand moments)**.** *The demand vector satisfies*

$$\mathbb{E}[d_t] = 0, \qquad \Sigma_d = \mathrm{Var}(d_t) \succ 0$$

with finite second moments. Moreover, Λ_t is independent of d_t and satisfies

$$\mathbb{E}[\Lambda_t^2] < \infty$$

Notation. *For $x \in \mathbb{R}^n$, x_k denotes the k-th component of x. For any generic matrix $V \in \mathbb{R}^{n\times n}$, V_{ij} denotes the (i,j)-th entry, $V_{i\bullet}$ its i-th row, and $V_{\bullet j}$ its j-th column. The symbol $\|\cdot\|_2$ denotes the Euclidean norm for vectors and the associated operator norm for matrices. For each k, let e_k denote the k-th canonical basis vector in $\mathbb{R}^n$.*

A.1. Proof of Proposition 1

Proof. From (1), the basis vector satisfies

$$b_t = K_t d_t = (T+\Phi)d_t + \Lambda_t \mathbf{1}\mathbf{1}' d_t = (T+\Phi)d_t + \Lambda_t S_t\,\mathbf{1}, \qquad S_t := \mathbf{1}' d_t.$$

Introduce a scaling parameter $M > 0$ and define a scaled stress process

$$\Lambda_t(M) := M\Lambda_t^0$$

where Λ_t^0 is the baseline stress, independent of d_t, with

$$\mu_0 = \mathbb{E}[\Lambda_t^0] < \infty, \qquad 0 < \nu_0 = \mathbb{E}\left[(\Lambda_t^0)^2\right] < \infty$$

For each M, define $K_t(M) = T + \Phi + \Lambda_t(M)\mathbf{1}\mathbf{1}'$ and

$$b_t(M) = K_t(M)d_t$$

Fix two currencies $i \neq j$. Denote the idiosyncratic contributions as

$$a_{i,t} := ((T + \Phi)d_t)_i, \quad a_{j,t} := ((T + \Phi)d_t)_j$$

so that

$$b_{i,t}(M) = a_{i,t} + \Lambda_t(M)S_t, \qquad b_{j,t}(M) = a_{j,t} + \Lambda_t(M)S_t.$$

Since $\mathbb{E}[d_t] = 0$, we have $\mathbb{E}[a_{i,t}] = \mathbb{E}[a_{j,t}] = \mathbb{E}[S_t] = 0$. Denote

$$\begin{aligned} v_i &= \mathrm{Var}(a_{i,t}), & v_j &= \mathrm{Var}(a_{j,t}), & c_{ij} &= \mathrm{Cov}(a_{i,t}, a_{j,t}) \\ u_i &= \mathrm{Cov}(a_{i,t}, S_t), & u_j &= \mathrm{Cov}(a_{j,t}, S_t), & v_S &= \mathrm{Var}(S_t) \end{aligned}$$

The proposition is meaningful when $v_S > 0$. Using independence of $\Lambda_t(M)$ and d_t, together with the zero-mean conditions above, we obtain the covariance and variances

$$\begin{aligned} \mathrm{Cov}(b_{i,t}(M), b_{j,t}(M)) &= c_{ij} + M^2\nu_0\, v_S + M\mu_0(u_i + u_j) \\ \mathrm{Var}(b_{i,t}(M)) &= v_i + M^2\nu_0\, v_S + 2M\mu_0\, u_i \\ \mathrm{Var}(b_{j,t}(M)) &= v_j + M^2\nu_0\, v_S + 2M\mu_0\, u_j \end{aligned}$$

$$\mathrm{Corr}\big(b_{i,t}(M), b_{j,t}(M)\big) = \frac{c_{ij} + M\mu_0(u_i + u_j) + M^2\nu_0 v_S}{\sqrt{\big(v_i + 2M\mu_0 u_i + M^2\nu_0 v_S\big)\big(v_j + 2M\mu_0 u_j + M^2\nu_0 v_S\big)}}.$$

As $M \to \infty$, the $\nu_0 M^2 v_S$ term dominates numerator and denominator. Dividing numerator and denominator by $\nu_0 M^2 v_S$ and taking the limit gives

$$\lim_{M\to\infty} \mathrm{Corr}\big(b_{i,t}(M), b_{j,t}(M)\big) = 1.$$

Thus, under sufficiently strong global funding stress, all basis spreads load predominantly on the same common factor S_t, producing near-perfect comovement. □

The term $\Lambda_t \mathbf{1}\mathbf{1}'$ is rank one and loads equally on all currencies through aggregate net USD demand S_t. When stress is moderate, bilateral and idiosyncratic components matter. When stress becomes sufficiently large, the common factor dominates, and basis spreads move together.

A.2. Proof of Proposition 2

Proof. Fix a currency k and consider a local demand perturbation

$$d_t \mapsto d_t + \xi e_k, \qquad \xi > 0$$

Holding K_t fixed at the instant of the shock, (1) implies

$$\Delta b_t = K_t(\xi e_k) = \xi K_t e_k$$

Therefore, the impact on currency j is $(\Delta b_t)_j = \xi (K_t)_{jk}$. For $j \neq k$, the diagonal matrix T contributes nothing, so

$$(K_t)_{jk} = \phi_{jk} + \Lambda_t$$

Thus, the aggregate effect on all other currencies is

$$\sum_{j\neq k}(\Delta b_t)_j = \xi\sum_{j\neq k}(\phi_{jk}+\Lambda_t) = \xi\sum_{j\neq k}\phi_{jk} + \xi(n-1)\Lambda_t$$

Define the balance-sheet centrality of currency k as $C_k = \sum_{j\neq k}\phi_{kj}$. Because $\Phi = \Phi'$, row and column sums coincide: $\sum_{j\neq k}\phi_{kj} = \sum_{j\neq k}\phi_{jk}$. By symmetry of Φ,

$$\sum_{j\neq k}\phi_{jk} = C_k, \quad \Rightarrow \quad \sum_{j\neq k}(\Delta b_t)_j = \xi C_k + \xi(n-1)\Lambda_t$$

Likewise, if the same perturbation hits another currency $i \neq k$, then

$$\sum_{j\neq i}(\Delta b_t)_j = \xi C_i + \xi(n-1)\Lambda_t$$

Hence

$$\sum_{j\neq k}(\Delta b_t)_j > \sum_{j\neq i}(\Delta b_t)_j \iff C_k > C_i$$

Since the common term $\xi(n-1)\Lambda_t$ cancels, relative transmission is governed solely by the centrality indices $\{C_k\}_{k=1}^n$. Therefore, currency k is the strongest transmitter of shocks if and only if C_k is maximal. □

A demand shock to currency k propagates through the kth column of the cost kernel K_t. The diagonal matrix T does not generate cross-currency effects, and the common term $\Lambda_t\mathbf{1}\mathbf{1}'$ affects all off-diagonal entries equally. Relative differences in outward transmission are therefore governed by the cross-currency linkage matrix Φ.

A.3. Proof of Proposition 3

To obtain a precise benchmark version of the proposition, we state explicitly the assumptions required for the pegged-currency result.

Assumption 3 (Hard-peg benchmark). *Fix a pegged currency k. Assume:*

(i) $d_{k,t} = 0$ *almost surely;*
(ii) $\phi_{kj} = 0$ *for all* $j \neq k$*;*
(iii) *for every non-pegged currency i, if $X_{i,t} = \tau_i d_{i,t} + \sum_{j\neq i}\phi_{ij}d_{j,t}$, $S_t = \mathbf{1}'d_t$, $Z_t = \Lambda_t S_t$, then* $\mathrm{Cov}(X_{i,t}, S_t) \geq 0$.
(iv) $\mathbb{E}[\Lambda_t] \geq 0$.

Assumption 3 describes an idealised hard-peg benchmark. The approximate statement for tightly managed pegs follows when conditions (i) and (ii) hold only approximately.

Proof. For the pegged currency k, the pricing relation (1) gives

$$b_{k,t} = \tau_k d_{k,t} + \sum_{j\neq k}\phi_{kj}d_{j,t} + \Lambda_t S_t$$

Under Assumption 3(i)–(ii), $b_{k,t} = Z_t = \Lambda_t S_t$ almost surely. Therefore

$$\mathrm{Var}(b_{k,t}) = \mathrm{Var}(Z_t)$$

Now consider any non-pegged currency i. Its basis can be written as

$$b_{i,t} = X_{i,t} + Z_t,$$

where $X_{i,t} = \tau_i d_{i,t} + \sum_{j \neq i} \phi_{ij} d_{j,t}$. Hence

$$\mathrm{Var}(b_{i,t}) = \mathrm{Var}(X_{i,t}) + \mathrm{Var}(Z_t) + 2\,\mathrm{Cov}(X_{i,t}, Z_t)$$

Because Λ_t is independent of d_t, and both $X_{i,t}$ and S_t are measurable functions of d_t, we have

$$\mathrm{Cov}(X_{i,t}, Z_t) = \mathrm{Cov}(X_{i,t}, \Lambda_t S_t) = \mathbb{E}[\Lambda_t]\mathrm{Cov}(X_{i,t}, S_t)$$

where we also used $\mathbb{E}[X_{i,t}] = \mathbb{E}[S_t] = 0$, which follows from Assumption 2. By Assumption 3(iii)–(iv), $\mathrm{Cov}(X_{i,t}, Z_t) \geq 0$. Therefore:

$$\mathrm{Var}(b_{i,t}) \geq \mathrm{Var}(Z_t) = \mathrm{Var}(b_{k,t})$$

Thus the basis of a hard-pegged currency is no more volatile than the basis of any non-pegged currency satisfying Assumption 3(iii). □

Approximate peg case. If $d_{k,t}$ and the row $\{\phi_{kj}\}_{j \neq k}$ are not exactly zero but are small in L^2, then the local term

$$\tau_k d_{k,t} + \sum_{j \neq k} \phi_{kj} d_{j,t}$$

is small in variance, so $b_{k,t}$ remains close to Z_t and therefore remains comparatively muted.

Under a hard peg, private agents in currency k generate little independent net USD demand, and dealers do not warehouse substantial bilateral non-USD exposures through that leg. The pegged currency, therefore, loads primarily on the common global stress component, whereas non-pegged currencies additionally carry local and network-specific variation.

A.4. Proof of Proposition 4

The maturity proposition requires a stronger structure than the previous propositions. We therefore make the required assumptions explicit. For each maturity $m \in \mathcal{M}$, denote

$$b_t^{(m)} = K_t^{(m)} d_t^{(m)}, \qquad K_t^{(m)} = T^{(m)} + \Phi^{(m)} + \Lambda_t \mathbf{1}\mathbf{1}'$$

with $T^{(m)} = \mathrm{diag}(\tau_1^{(m)}, \ldots, \tau_n^{(m)})$, $\Phi^{(m)} = \Phi^{(m)\prime}$.

Assumption 4 (Demand representation across maturities)**.** *For each maturity m, there exists a mean-zero vector of currency-indexed primitive shocks $\xi_t = (\xi_{1,t}, \ldots, \xi_{n,t})'$ with covariance matrix $\Sigma_\xi \succeq 0$, independent of Λ_t, and a deterministic matrix $H^{(m)}$ such that*

$$d_t^{(m)} = H^{(m)} \xi_t.$$

Define $Q_t^{(m)} = K_t^{(m)} H^{(m)}$, then

$$b_t^{(m)} = Q_t^{(m)} \xi_t$$

Assumption 5 (Long-tenor contraction)**.** *If $m_2 > m_1$, let*

$$A_t^{(m)} := Q_t^{(m)} \Sigma_\xi^{1/2},$$

where $\Sigma_\xi^{1/2}$ is any symmetric positive-semidefinite square root of Σ_ξ. Assume that there exists a contraction matrix $R_t^{(m_2,m_1)}$ satisfying

$$\|R_t^{(m_2,m_1)}\|_2 \leq 1$$

such that

$$A_t^{(m_2)} = A_t^{(m_1)} R_t^{(m_2,m_1)}.$$

Equivalently,

$$Q_t^{(m_2)} \Sigma_\xi^{1/2} = Q_t^{(m_1)} \Sigma_\xi^{1/2} R_t^{(m_2,m_1)}.$$

Assumption 6 (Row-wise off-diagonal contraction)**.** *For each currency k and each pair $m_2 > m_1$, let*

$$P_{-k} = I - e_k e_k'$$

Assume that there exists a contraction matrix $R_{k,t}^{(m_2,m_1)}$ satisfying

$$\|R_{k,t}^{(m_2,m_1)}\|_2 \leq 1$$

such that $e_k' Q_t^{(m_2)} P_{-k} = e_k' Q_t^{(m_1)} P_{-k}\, R_{k,t}^{(m_2,m_1)}$.

Assumption 5 formalises the net attenuation of the equilibrium transmission mechanism at longer maturities. It allows higher long-tenor inventory costs to coexist with lower long-tenor volatility provided that weaker client demand and attenuated cross-currency warehousing are sufficiently strong to reduce the covariance-weighted transmission map.

Proof. By Assumption 4,

$$b_t^{(m)} = Q_t^{(m)} \xi_t$$

Conditional on Λ_t,

$$\text{Var}(b_t^{(m)} \mid \Lambda_t) = Q_t^{(m)} \Sigma_\xi Q_t^{(m)\prime}.$$

Fix two maturities $m_2 > m_1$ and define

$$A_t^{(m)} = Q_t^{(m)} \Sigma_\xi^{1/2},$$

where $\Sigma_\xi^{1/2}$ denotes the symmetric positive-semidefinite square root of Σ_ξ. Then

$$\text{Var}(b_t^{(m)} \mid \Lambda_t) = A_t^{(m)} A_t^{(m)\prime}.$$

By Assumption 5,

$$A_t^{(m_2)} = A_t^{(m_1)} R_t^{(m_2,m_1)}, \qquad \|R_t^{(m_2,m_1)}\|_2 \leq 1.$$

Since $\|R_t^{(m_2,m_1)}\|_2 \leq 1$,

$$R_t^{(m_2,m_1)} R_t^{(m_2,m_1)\prime} \preceq I.$$

Hence

$$\begin{aligned}
\mathrm{Var}(b_t^{(m_2)} \mid \Lambda_t) &= A_t^{(m_2)} A_t^{(m_2)\prime} \\
&= A_t^{(m_1)} R_t^{(m_2,m_1)} R_t^{(m_2,m_1)\prime} A_t^{(m_1)\prime} \\
&\preceq A_t^{(m_1)} A_t^{(m_1)\prime} \\
&= \mathrm{Var}(b_t^{(m_1)} \mid \Lambda_t).
\end{aligned}$$

Taking expectations over Λ_t preserves Loewner order, so

$$\mathrm{Var}(b_t^{(m_2)}) \preceq \mathrm{Var}(b_t^{(m_1)}).$$

In particular, for each currency k,

$$\mathrm{Var}(b_{k,t}^{(m_2)}) \leq \mathrm{Var}(b_{k,t}^{(m_1)}).$$

Turning to spillovers. Define the off-diagonal row loading of currency k at maturity m by

$$\Gamma_{k,t}^{(m)} = e_k' Q_t^{(m)} P_{-k}$$

By Assumption 6, $\Gamma_{k,t}^{(m_2)} = \Gamma_{k,t}^{(m_1)} R_{k,t}^{(m_2,m_1)}$. Hence

$$\|\Gamma_{k,t}^{(m_2)}\|_2 = \|\Gamma_{k,t}^{(m_1)} R_{k,t}^{(m_2,m_1)}\|_2 \leq \|\Gamma_{k,t}^{(m_1)}\|_2 \|R_{k,t}^{(m_2,m_1)}\|_2 \leq \|\Gamma_{k,t}^{(m_1)}\|_2$$

$$\therefore \ \|e_k' Q_t^{(m_2)} P_{-k}\|_2 \leq \|e_k' Q_t^{(m_1)} P_{-k}\|_2$$

Since $e_k' Q_t^{(m)} P_{-k}$ is exactly the row-k loading on non-k shocks, this establishes weaker cross-currency spillovers at the longer maturity. □

The matrix $Q_t^{(m)} = K_t^{(m)} H^{(m)}$ is the equilibrium transmission operator that maps exogenous shocks into basis movements. The contraction assumptions state that once one combines higher long-tenor inventory costs, weaker long-tenor demand, and attenuated cross-currency warehousing, the overall transmission map becomes weaker at longer maturities. Under those conditions, both basis volatility and outward spillovers decline with maturity.